Journal of Advanced Research in Fluid Mechanics and Thermal Sciences 49, Issue 2 (2018) 101-114

Penerbit Akademia Baru

Journal of Advanced Research in Fluid Mechanics and Thermal Sciences

Journal homepage: www.akademiabaru.com/arfmts.html
ISSN: 2289-7879

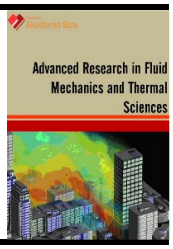

Numerical Simulation on Wind-Driven Cross Ventilation in Square Arrays of Urban Buildings with Different Opening Positions

Open Access

Sheikh Ahmad Zaki[1,*], Nur Farhana Mohamad Kasim[1], Naoki Ikegaya[2], Aya Hagishima[2], Mohamed Sukri Mat Ali[1]

[1] Malaysia-Japan International Institute of Technology, Universiti Teknologi Malaysia, Kuala Lumpur 54100, Malaysia
[2] Interdisciplinary Graduate School of Engineering Sciences, Kyushu University, 6-1 Kasuga-Koen, Kasuga-shi, Fukuoka 816-8580, Japan

ARTICLE INFO

Article history:
Received 21 June 2018
Received in revised form 31 August 2018
Accepted 2 September 2018
Available online 10 September 2018

ABSTRACT

Effective wind-driven cross ventilation requires a well-designed opening, such as a window, to allow sufficient exchange between indoor and outdoor air, especially when the building is surrounded by other buildings. Using computational fluid dynamics, the present study investigated the effect of different opening positions on wind-driven ventilation in a building in an area with a packing density of 25%. The renormalization-group κ–ε turbulence model, a type of Reynolds-averaged Navier–Stokes (RANS) model, was used to characterize the airflow in cubical building blocks arranged in a square array. Nine different configurations of aligned cross openings and nine configurations with non-aligned outlet positions were tested. The ventilation rates obtained for the aligned cross openings showed that openings positioned at the uppermost of the windward and leeward façade provided highest ventilation rate. The ventilation rate was reduced by 75% when the openings were positioned at the bottom of the façade. As for the fixed inlet in the centre, the ventilation rate was 100% higher when the outlet is at the top of the leeward façade compared to the bottom of the façade. The outcomes of this study show that opening position is imperative in providing effective wind-driven cross ventilation in urban areas.

Keywords:
Wind-driven cross ventilation, opening position, square array, Reynolds-averaged Navier–Stokes (RANS) model, ventilation rate

1. Introduction

Wind-driven cross ventilation is one of the alternative strategies that are widely acknowledged for overcoming the effect of urban heat islands (UHIs) for a more sustainable environment in urban area. It has been shown to provide effective ventilation not just in isolated buildings, but also in buildings surrounded by other buildings [1]. However, wind-driven cross ventilation in a densely packed area (i.e. urban or suburban area) can be less effective owing to the lower wind speed, UHIs,

* *Corresponding author.*
E-mail address: sheikh.kl@utm.my (Sheikh Ahmad Zaki)

local noise, and air pollution [2]. Furthermore, the presence of surrounding buildings including the geometry could significantly affect the distribution of surface pressure on the building wall, which is the main parameter in the calculation of the ventilation rate, as the air flow is somewhat modified by the effect of building interference [3-4]. In a wind-tunnel study, the cross-ventilation rate was reduced by approximately 70% when a small pressure difference existed between the windward and leeward walls of a building that was sheltered on all sides by other buildings without openings [5]. Another computational study also showed that taking the surrounding buildings into account when estimating wind-driven ventilation can result in a difference of up to 96% in the air change rate per hour (ACH) [6]. In addition, increasing the aspect ratio of a street canyon leads to a reduction in the cross-ventilation rate [7] because the pressure difference between the windward and leeward walls is reduced when the buildings are closely packed together [8]. On the contrary, a numerical study on high-rise buildings with cross openings suggested that arranging the buildings in a staggered configuration can provide better wind-driven ventilation in such crowded area [9]. The findings of this study also indicated that the ventilation rate varies with the wind direction.

Apart from that, indoor ventilation can also be improved by controlling the window openings according to the indoor and outdoor conditions [10]. Many cross-ventilation studies have focused on the design, including the position, size, and geometry, of openings. Using CFD, Seifert *et al.*, [11] have extensively studied the effects of opening location, wall porosity, and wall thickness. The study mentioned that placing the opening on the upper level of a building with wall porosity of >10% can accelerate the airflow rate. In addition, the inlet-to-outlet ratio should also be considered in cross-ventilation prediction [12]. Openings with an inlet-to-outlet ratio of less than unity can introduce indoor air with velocity which could influence the level of thermal comfort inside the building. In an isolated building, multiple openings on both windward and leeward façades can enhance the ventilation and provide uniform mixing inside the building if there is a large gap between these openings [13]. Nonetheless, published works on openings are limited to those in isolated buildings over a simplified interior of building rather than the more realistic condition in which the target building is surrounded by neighbourhood buildings. A few studies have reported the influence of surrounding buildings on indoor ventilation. For example, Tominaga and Blocken [5] performed wind tunnel experiment for investigating the effect of the surrounding buildings on cross ventilation of fixed opening with packing density of 25%. They found that the ventilation rate was reduced approximately 30% compared to isolated building due to the presence of surrounding buildings. However, it is still inadequate information since the systematic studies have not been performed with various position of opening configurations in urban buildings array.

Hence, the present study aims to reveal the relationship between opening configurations (i.e. positions) and ventilation in a building within a large group of constructions by performing a CFD simulation with a three-dimensional steady-state Reynolds-averaged Navier–Stokes (RANS) equation. Most of the existing computational studies are conducted on a single building model [11-14] or building surrounded by other buildings [6,7,9,15] using the computational domain with the criteria suggested by the best practise guideline [16], with inlet boundary condition adopted from wind tunnel study. However, in simulating flow over a large building group, a periodic boundary condition can be used instead of a large computational domain in order to reduce the computational cost [17]. This boundary condition has been widely applied in the study of flow over cubical array to investigate various parameters such as flow characteristic and wind surface pressure distribution on buildings [18-20]. Nevertheless, the use of periodic boundary condition in simulating wind-induced cross ventilation in large group of buildings is scarce which is also due to the insufficiency of wind-induced cross ventilation study in urban area.

In the present study, nine configurations of aligned cross openings on the windward and leeward façades were tested to evaluate the effect of different opening positions. Additionally, the effect of outlet position was also investigated by fixing the inlet on the central part of the windward façade and varying the outlet position on the leeward façade. Even though the ventilation rates are generally dependent on the approaching wind direction, the area packing density and the buildings arrangement, these parameters were fixed (as described in the next section) in the present study because the main focus was to investigate the effect of opening position.

2. Methodology

2.1 CFD Simulation

2.1.1 Computational domain

The computational domain was constructed to represent an infinitely repeating unit with an area packing density, λ_p, of 25%, defined by the ratio of total plan area of the building, A_p to the total plan area of the floor, A_s. The size of the domain was $2H$ (L_x) × $2H$ (L_y) × $4H$ (L_z), where H is the building height, and L_x, L_y, and L_z are the lengths in the streamwise (x, parallel to the direction of airflow), spanwise (y, perpendicular to the direction of airflow), and vertical (z) directions, respectively, as illustrated in Figure 1.

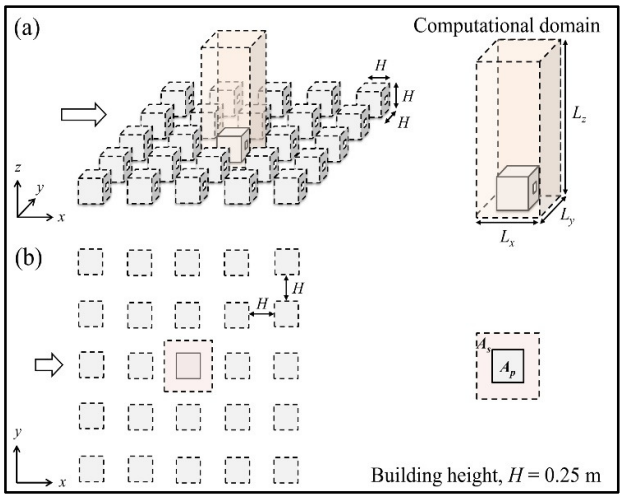

Fig. 1. Computational domain: (a) schematic view; (b) plan view

A uniform Cartesian grid was applied in the present study. A grid-independence study was also conducted based on three grid resolutions – coarse, medium, and fine. A simplified cubic building model with a height of H = 0.25 m was placed in the centre of the computational domain. We selected this scale dimension that corresponding to the wind tunnel experiments could be conducted in the future to confirm the simulation results. The actual dimension should be at the scale of 1:40. The building model was constructed with cross openings, where the inlet was located on the windward façade and the outlet was on the leeward façade; the dimensions of the openings are shown in Figures 2(a) and 2(b) presented the possible opening positions to be evaluated in the present study. The size of each opening for a wall porosity of 8% was calculated from the ratio of the area of the opening to the area of the building wall ($A_{opening}/A_{wall}$); these openings are considered to be small

ones according to Seifert *et al*., [11]. In this simulation we only considered the fixed size of opening with simplified building shape and array, and focus on the influence of opening positions.

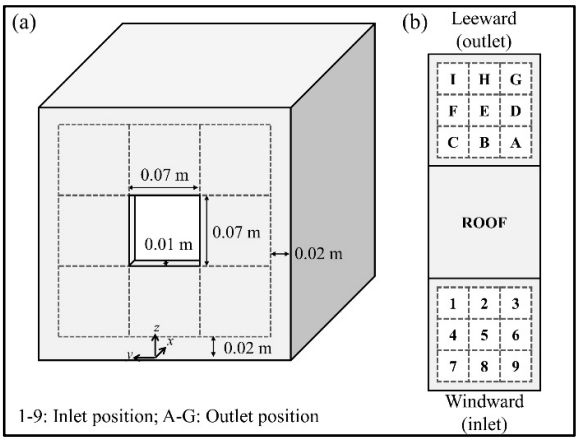

Fig. 2. Building model: (a) dimensions of opening; (b) possible locations of opening

For cases with aligned cross openings (see Figure 3), both inlet (represented by numerals 1 to 9) and outlet (represented by alphabets A to G) were placed directly opposite to each other. For cases with different outlet positions (see Figure 4), the inlet was fixed at position number 5 while the outlet position was varied from location A to G in each case.

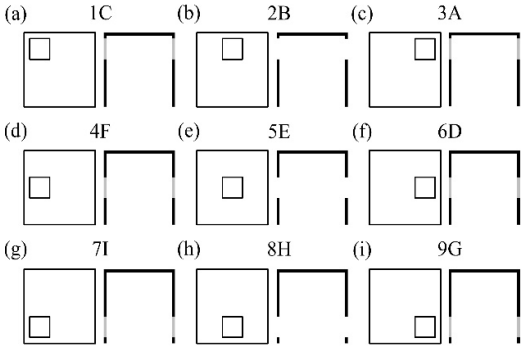

Fig. 3. Front (left) and side (right) view of configurations for aligned cross openings.

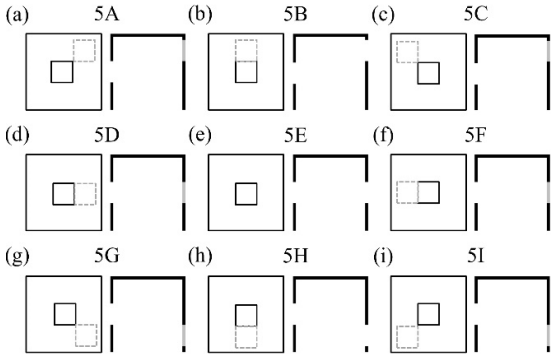

Fig. 4. Front (left) and side (right) view of configurations for different outlet positions.

2.1.2. Boundary conditions

The simulations in the present study were conducted using an open-source software package called OpenFOAM (version 2.2.1) (OpenFOAM 2013). The renormalization-group (RNG) κ–ε turbulence closure model [21] was employed, where κ represents the turbulence kinetic energy and ε represents the turbulence dissipation rate; the flow field equations were solved using the SIMPLE method for pressure–velocity coupling [22]. All the simulations are carried out under the isothermal condition and the flow is assumed to be incompressible and steady state. The convergence of the flow fields were obtained when all the scaled residuals reached a minimum of 10^{-7} for *x* velocity, 10^{-5}

for y and z velocity as well as κ and ε. The convergence criteria are set to comply with the recommended constant residuals of 10^{-4} or less for all residuals [16,23]. The prevailing wind was assumed to flow at 0°, which is normal to the opening. The inflow is induced by a pressure gradient source, $\nabla p = \rho u^*/L_z$ where ρ is the air density, u^* is the friction velocity and L_z is the domain height, based on a mean flow velocity, U of 8 m/s. The pressure gradient is calculated to adjust the volume averaged velocity in the whole domain to the desired mean velocity, U. The wind speed measured at a building height of H yielded an approximate Reynolds number ($Re_b = U_H H/\nu$) of 80,000 for the building, where U_H is the reference velocity at H, and ν is the kinematic viscosity. Additionally, the Reynolds number of airflow through the opening, $Re_o = U_o D_o/\nu$, ranged from 600 to 5000 for different configurations, where the parameter U_o represents the velocity at the opening, and D_o represents the length of the opening. These Reynolds numbers are higher than those previously reported by Cermak *et al.,* [24] for a Reynolds-number-independent flow, where $Re_b > 20{,}000$ for flow around a bluff body and $Re_o > 300$ for flow through an opening.

Periodic boundary condition that is defined by the terms "*cyclic*" in OpenFOAM are imposed in both streamwise and spanwise direction to resemble a flow over large building groups as in urban area, see Figure 1. This type of boundary condition is usually used for simulating repeating geometries infinitely where it implies that all variables on the outflow boundary from the previous step of calculation are imposed on the inflow boundary in the next step calculation. Since the RANS equation only provides a time-averaged solution, the horizontal area ($L_x \times L_y$) of the computational domain, which was $2H \times 2H$ in this study, is considered sufficient for capturing the mean flow properties [20]. A non-slip boundary condition and a wall function based on the roughness height, K_s, and roughness constant, C_s, were applied to the domain floor (i.e. ground surface) and building surfaces. The values of 0.001 for K_s and 0.5 for C_s for the ground surface were selected in this study to produce a roughness height of $z_0 = 5 \times 10^{-5}$. The values were based on the following expression [25].

$$z_O = \frac{C_S K_S}{E} \tag{1}$$

where E is an empirical constant with a value of 9.8. The top boundary of the domain is treated as a free slip condition.

2.2 Preliminary Simulation

To the extent of the authors' knowledge, the configuration of the simulation model proposed in the present study has not been used in any wind-tunnel experiment. Therefore, the first part of this preliminary simulation was carried out on a cubical solid block without opening as the closest comparable case to validate the accuracy of periodic boundary condition used in the present study. This preliminary simulation was performed to determine the best RANS closure model by comparing the results with earlier studies which used a direct numerical simulation (DNS) with higher-order accuracy that has been successfully validated against a wind tunnel study. The second part of the simulation involved the building with openings, and it included sensitivity evaluation of the effect of different grid resolutions. All the simulations in the preliminary stage were conducted using the computational settings described in section 2.

2.2.1 Impact of turbulence models: Building with solid walls

The selection of a turbulence model has a significant impact on the numerical errors and uncertainties which could affect the accuracy of the results. Thus, three types of RANS models,

namely RNG, realizable κ–ε (RKE), and shear–stress transport κ–ω (SST), were used in the sensitivity study to confirm the reliability of each closure model in predicting wind-driven cross ventilation. The simulations for each turbulence model were conducted using a grid resolution of *H*16 ('16' refers to the number of grid cells per building with height of *H*) that consists of 56,320 cells and a domain height of 4*H*. The use of finer grids and further extension of the domain height did not modify the spatially averaged profiles near the area of interest (i.e. below the canopy). As shown in Figure 5, the results of the spatially averaged mean-velocity over the entire horizontal plane (*x*-*y*) of the computational domain, U_s, were compared with those of a previous study using a DNS model by Coceal *et al*., [19]. This comparison is intended to assess the capability of the RANS models used in the present study with periodic boundary condition in simulating flow over large group of buildings. The results were normalized against the respective spatially averaged mean velocity at a height of *Z*, with $Z/H = 2$. The mean velocity captured by the RANS models shows an underestimation in the lower half of the canopy. Moreover, the limitation of RANS models in accurately predicting the vortex in the street canyon resulted in negative values of spatially averaged velocity near the ground due to domination of reversing flow. On the other hand, larger discrepancies were also observed near the floor, especially when compared to the SST model. In addition, all three models overestimated the mean velocity near the top of the canopy, with a larger difference exhibited by the SST model. A comparison of the RANS and DNS results showed the former were consistent with those of an earlier study on the limitation of the RANS model in obtaining the mean air velocity within a building array [20]. Despite the limitation, all RANS models sufficiently reproduced the general patterns of the profiles. Hence, RANS is still considered reliable for investigating the airflow behaviour in cubical arrays and is believed to adequately serve the purpose of this study. Among the RANS models, RNG was chosen for the remaining tests because of its reasonable accuracy, computational cost, and most importantly, superior performance in cross-ventilation prediction in previous studies [11,14,26].

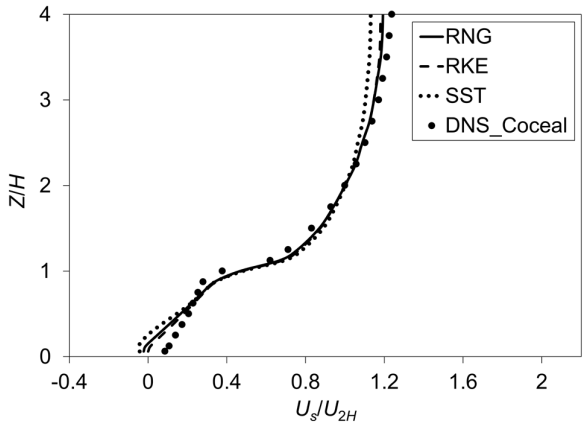

Fig. 5. Normalized spatially averaged velocity profiles, U_s/U_{2H}, for different turbulence models. 'DNS_Coceal' refers to the square array DNS data obtained by Coceal *et al*., [19]

2.2.2 Impact of grid resolution: building with openings

In the case of a building with openings, a uniform structured grid with a size of *H*25 which is constructed from 234,669 cells was selected as the coarse grid. The number of grids was slightly

higher than the minimum of ten grid cells per cube root of building volume suggested in the best practice guidelines [16]. The grid was then refined by a factor of two to medium resolution and fine resolution that are *H*50 (879,810 cells) and *H*100 (1,459,305 cells), respectively to satisfy the grid-refinement criterion [23]. The convergence of the grid calculations was determined based on a comparison of the normalized ventilation rates, Q/Q_{ref}, obtained at the opening, where Q is the ventilation rate calculated from the integration of air velocity at the opening [27].

$$Q = \frac{1}{2}\sum_{j=jm}^{jn}\sum_{k=km}^{kn}\left|U_{j,k}\right|\Delta y_j \Delta z_k \tag{2}$$

In Equation (2), $U_{j,k}$ is the mean velocity normal to the grid (Δy_j, Δz_k) at the opening, and [Δy_{jm}, Δy_{jm+1}, …, Δy_{jn}] and [Δz_{km}, Δz_{km+1}, …, Δz_{kn}] are the grid sizes within the opening. The absolute-value notation for the velocity $U_{j,k}$ indicates the summation of both inflow and outflow of air in the building. However, as $Q_{in} = Q_{out}$, the ventilation rate, Q, is corrected by a factor of '1/2' in the equation. On the other hand, Q_{ref} is the reference ventilation rate defined by U_H (velocity U obtained at a building height of H) × $A_{opening}$ (area of the opening). Based on the results shown in Figure 6, the grid sensitivity was most significant inside the building in the area downstream of the inlet (represented by a distance X along the x direction, where X/H = 0–0.8).

The ventilation rates presented in Figure 7 shows that the percentage difference between the normalized ventilation rates for grid sizes *H*25 and *H*100 was about 21%, while that for grid sizes *H*50 and *H*100 was approximately 0.7%. Since a finer grid did not yield any significant difference in the ventilation rate, the medium grid resolution (*H*50) was considered sufficient and was selected for the rest of the study.

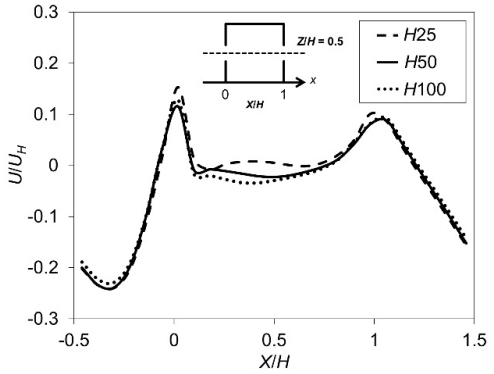

Fig. 6. Normalized velocity profiles along the horizontal line for different grid resolutions

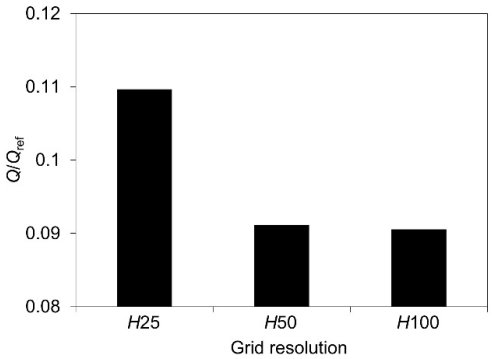

Fig. 7. Normalized ventilation rates for different grid resolutions

3. Results and Discussion

3.1 Flow Distribution

3.1.1 Building with aligned cross openings

The effect of openings positions on airflow distribution inside building was further analysed based on the velocity vectors and contours of configurations 2B, 5E, and 8H presented in Figure 8. Higher velocity was observed at X/H = 0 for 2B owing to strong incoming airflow penetrating the opening in the upper part. The size of the air stream (jet) flowing through the inlet was also wider for 2B than

for 5E and 8H. A downwards penetrating inflow (attributed to the vortex upstream of the opening) and a small recirculation flow below the jet were observed for both configurations 2B and 5E. The openings positioned in the lower part of the building (e.g. 8H) experienced weaker ventilation because the incoming airflow near the inlet flowed vertically downwards and almost parallel to the windward façade. Furthermore, the separating flows from the building near the bottom part of the upstream canyon also restricted the amount of air entering the lower openings. In configurations 5E and 8H, the airflow leaving the outlet was driven by the recirculating flow in the downstream canyon and was therefore directed upwards, which is in contrast to the exiting airflow in configuration 2B. In addition, it is also worth mentioning that a larger calm zone (with air velocity of nearly zero) was observed in the upper half of the indoor space when the openings were located at the lower level of the building.

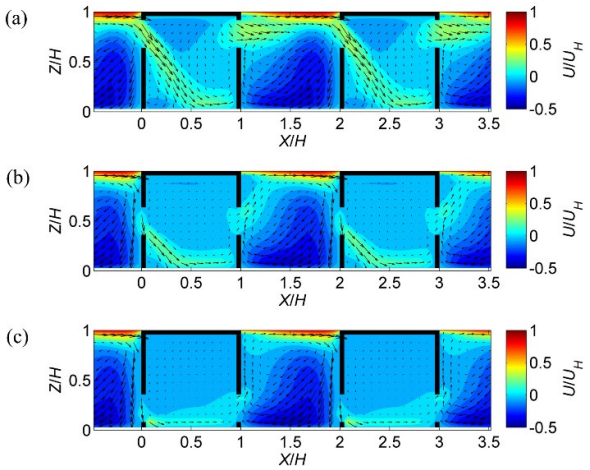

Fig. 8. Velocity contours and vectors for three different opening configurations: (a)2B; (b) 5E; (c) 8H

Contrary to the other cases, the flow in configuration 7I entered the building through the leeward opening and exited through the windward opening, as shown in Figure 9. The direction of airflow is defined by the counter-rotating vortex pair in the horizontal plane at Z/H = 0.22 (centre height of the opening) between the building blocks, where it tended to create larger suction (flow separated from the building) on the upstream opening.

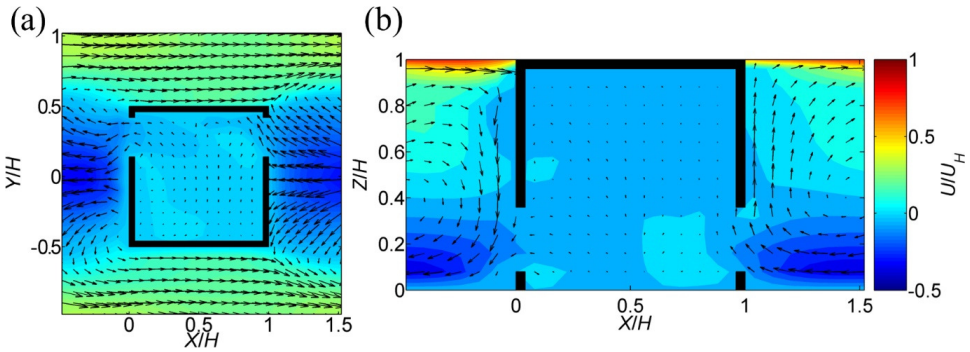

Fig. 9. Velocity contours and vectors for configuration 7I: (a) plan view; (b) side view

Figure 10 shows the spanwise distribution of airflow inside the building for all six cases, obtained by measuring the normalized velocity at five sampling locations with X/H = 0.5. Configuration 1C showed higher wind velocity at sampling locations y2, y3, and y4 in the lower half of the building interior. Although location y1 was in the middle between the inlet and outlet of 1C, a weaker wind speed with average dimensionless velocity of about 0.01 was observed, compared to 0.08 at location y2. This indicates that the entering airflow was diverted towards the centre part rather than the lateral part of the building. The velocity profiles for the cases with openings located in the central area of the building façade (i.e. 2B, 5E, and 8H) showed their highest peak of dimensionless velocity at sampling location y3 in the area below Z/H = 0.4. At this location, the maximum velocity of 0.27 was exhibited by 5E, followed by 2B and then 8H. They also exhibited almost symmetrical profiles at locations y2 and y4, and locations y1 and y5, which indicate that the airflow was evenly distributed in the spanwise direction. Apart from that, as expected, configuration 7I exhibited weak velocity at all locations, thus justifying the low ventilation rate at the opening in Figure 8. In general, all cases showed higher air velocity in the lower half of the building, and the velocity gradually became nearly zero in the upper half because the entering airflow was directed downwards in most of the cases. Negative values were also observed near the top of the ceiling owing to air moving in the opposite direction as the flow circulated inside the building.

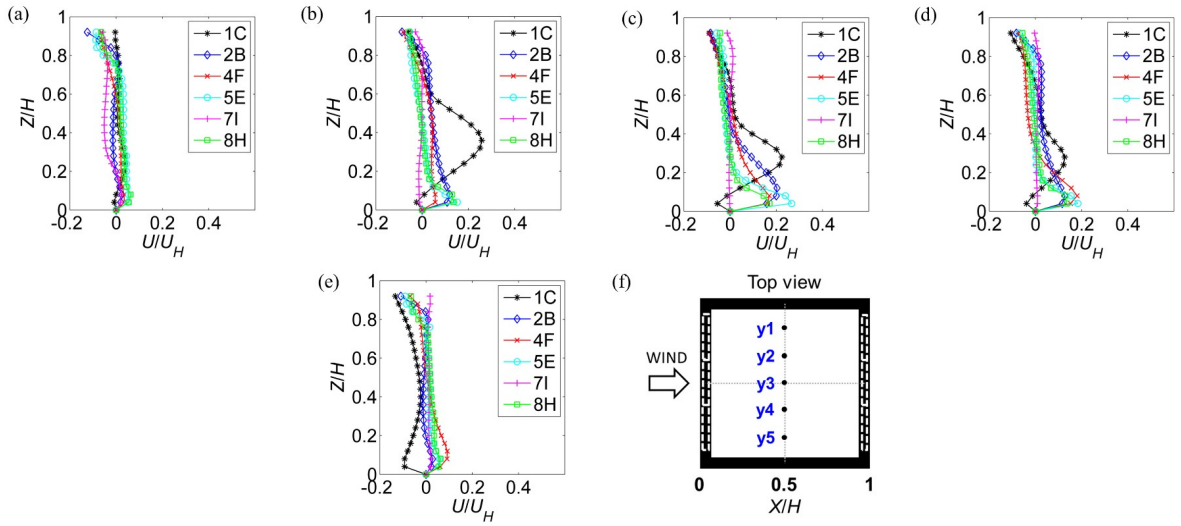

Fig. 10. Spanwise flow distribution inside building for cases with aligned cross openings: (a) location y1; (b) location y2; (c) location y3; (d) location y4; (e) location y5; (f) sampling locations

3.1.2 Effect of different outlet positions

The effect of different outlet positions was further investigated by comparing the velocity profiles at the inlet opening. The velocities obtained at the centre of the inlet opening along the height at Z/H = 0.36 to 0.64 (dotted line) are plotted in Figure 11. Configurations 5A and 5B exhibited similar profiles since they had nearly identical ventilation rates. The average dimensionless velocity of configuration 5D decreased by 4% from those of the first two configurations (5A and 5B), while the velocity was attenuated by 12.5% for configuration 5E. Further reduction by up to 64% was observed when the outlet was shifted from position in as configuration 5E to a lower level of the building (i.e. configurations 5G and 5H).

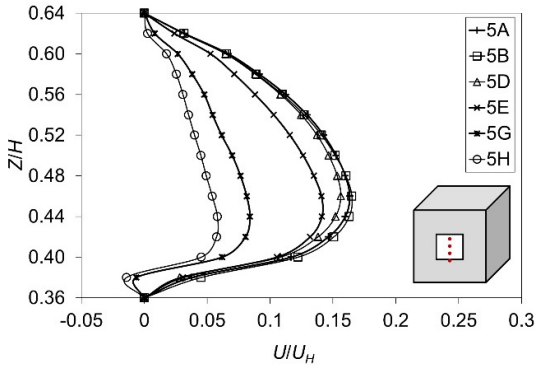

Fig. 11. Normalized velocity profiles at a fixed inlet opening (at position 5) but with the outlet located at different positions

Figure 12 presents the velocity contours and vectors for three different outlet positions in configurations 5B, 5E, and 5H. The flow inside the building and the downstream canyon was significantly modified, while it was less pronounced in the upstream canyon. The intensity of air velocity in the jet also weakened as the outlet was shifted to the lower part of the leeward façade. Figure 13 shows the spanwise distributions of indoor flow sampled at five different locations with X/H = 0.5 for all six cases with different outlet positions. The configurations with symmetrical airflow were excluded. Generally, higher velocity was observed at all sampling locations with Z/H below 0.2 because the penetrating flow was directed downwards, while the flow velocity in the upper area for all cases was nearly zero. Location y3 showed the highest dimensionless velocity, with a maximum value of 0.3 at the point just above the ground (Z/H = 0.04) for configurations 5A and 5B, where the outlet was positioned at the upper level of the leeward wall.

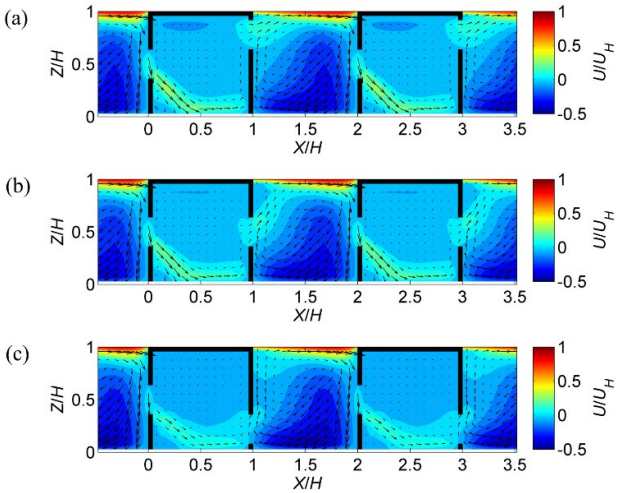

Fig. 12. Velocity contours and vectors for configurations with different outlet positions: (a) 5B; (b) 5E; (c) 5H

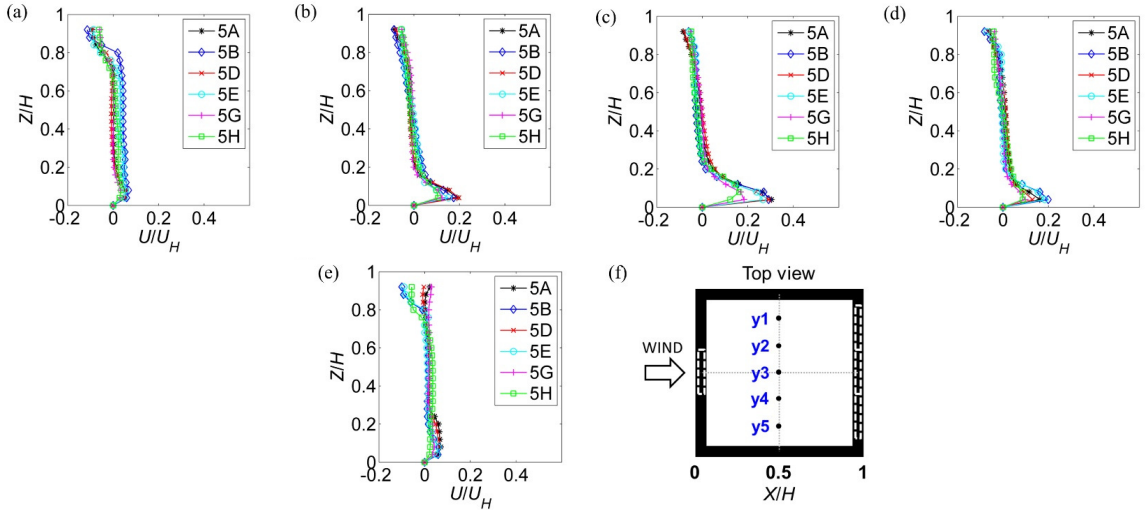

Fig. 13. Spanwise flow distribution inside a building for cases with different outlet positions: (a) location y1; (b) location y2; (c) location y3; (d) location y4; (e) location y5; (f) sampling locations

3.2 Ventilation Rate

The effect of the opening position was first investigated with different positions for the aligned cross openings. For inlet located at position '5', the corresponding outlet was shifted among nine different positions to investigate the effect of different outlet locations. The normalized ventilation rates for all configurations of both aligned and non-aligned openings were obtained by integrating the velocity at each opening. Identical ventilation rates were observed when openings were located on the lateral side of the building façade (i.e. 1C and 3A, 4F and 6D, 7I and 9G, 5A and 5C, 5D and 5F, 5G and 5I). These identical values can be explained by the symmetrical pressure distribution on building surfaces when the approaching wind is normal to the building front wall (i.e. windward) [18, 28]. In addition, the flow distribution at an intermediate height of the building showed a symmetrical pattern for configurations 4F and 6D. Therefore, the results for configurations 3A, 6D, 9G, 5C, 5F, and 5I will not be further analysed here. Figure 8 shows the ranking of ventilation performance in terms of ventilation rate for the remaining 11 cases and the isolated case conducted using a wind tunnel [5] and RNG turbulence model [29]. The ventilation rate exhibited a reduction of nearly 90% from the isolated case when the building with lower openings is surrounded by other buildings as in the present study. These results correspond to the findings reported by previous studies on the sheltering effect by surrounding buildings on wind-induced ventilation [5-6]. In the present study, higher ventilation rate was observed when the cross openings were aligned at the upper level of the building (e.g. 1C) with approximately 50% reduction from isolated case. The flow rate was decreased by 76% when the openings were positioned at the lower level (e.g. 7I). In addition, the effect of different outlet positions can also be seen in Figure 14. Configuration 5E was selected for reference since it consisted of an aligned configuration of openings that were also located at the centre of the building façade. Shifting the outlet to an upper position on the leeward façade slightly increased the ventilation rate by 14% from that of the reference case. In contrast, a maximum reduction of 44% was observed when the outlet was positioned near the bottom part of the leeward façade. These results are also consistent with existing findings on the surface pressure distribution on a building façade with a packing density of 25%, where the upper part of the wall tends to have higher pressure [18]. Moreover, the range of packing density used in the present study generated a skimming flow regime, in which the bulk of the flow did not enter the canyon [30] and the vortex core of the

recirculation flow inside the canyon was closer towards the top of the canyon. Therefore, an inlet at the upper level of the building tended to receive more air than one at the lower level.

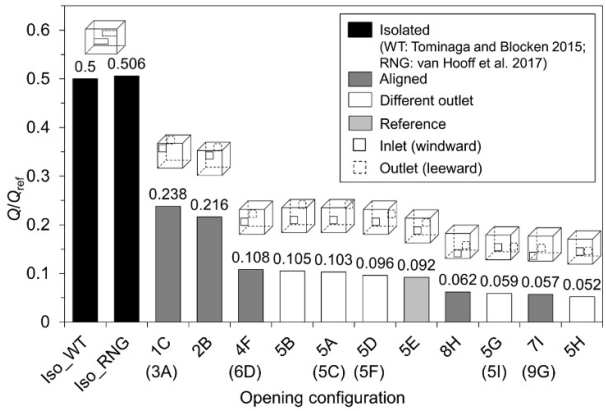

Fig. 14. Ranking of ventilation rate

3.3 Limitations of the Present Study

It is important to note the limitations of the present study. These limitations should be addressed in future phases of this research. The periodic boundary condition applied to the domain assumes that the surrounding buildings had identical opening configurations for all buildings as well as having uniform height; however, these settings do not represent a real urban environment. Thus, an extensive study on the effect of surrounding buildings' configurations is also necessary. In the present study, only a single wind direction, which is parallel to the opening, was considered, and the ventilation rate was estimated based on the mean flow properties while the effect of the fluctuating component was neglected. We also not considered the interior wall inside the building. Additionally, the buoyancy effect generated by the temperature difference between indoor and outdoor air was excluded as the study was essentially focused on ventilation driven by wind force. The various surrounding and shape of building conditions, and different interior wall configurations that more realistic will be discussed in future work.

4. Conclusions

Utilizing CFD methods, a series of simulations with various opening configuration was performed with the RANS RNG model to investigate the effect of different opening positions on cross ventilation in a building surrounded by other buildings, such as those found in an urban area. The following conclusions can be drawn.

(1) The opening located in the uppermost of the building provided up to 76% higher ventilation than the lower opening for aligned cross openings. On the other hand, shifting the outlet position either enhanced or attenuated the ventilation rate. For instance, the ventilation rate for an inlet positioned in the central part of the building was increased by nearly 14% when outlet position is closer to the top of building. However, the ventilation rate suffered a reduction of 44% with lower outlet.
(2) The structure of the standing vortex inside the canyon affected the airflow direction and the intensity of air velocity entering and exiting the building.
(3) The position of an opening also determined the uniformity of airflow distribution inside the building, which is important for a comfortable living environment.

In conclusion, the present study explored the fundamental relationship between airflow in building arrays and the positions of openings. Notwithstanding the shortcomings, the findings contribute to the field of wind-driven cross ventilation in the pursuit of sustainable urban development, especially for buildings in large groups.

Acknowledgement
This research is supported by the Malaysian Ministry of Higher Education (MOHE) under the Research University Grant (07H09) and Fundamental Research Grant Scheme (4F598) projects of Universiti Teknologi Malaysia.

References

[1] Niachou, Katerina, Samuel Hassid, Mat Santamouris, and Iro Livada. "Comparative monitoring of natural, hybrid and mechanical ventilation systems in urban canyons." *Energy and Buildings* 37, no. 5 (2005): 503-513.
[2] Ghiaus, Christian, Francis Allard, M. Santamouris, C. Georgakis, and F. Nicol. "Urban environment influence on natural ventilation potential." *Building and environment* 41, no. 4 (2006): 395-406.
[3] Khanduri, A. C., T. Stathopoulos, and Claude Bédard. "Wind-induced interference effects on buildings—a review of the state-of-the-art." *Engineering structures* 20, no. 7 (1998): 617-630.
[4] Mohammad, Ahmad Faiz, Sheikh Ahmad Zaki, Mohamed Sukri Mat Ali, Hagishima Aya, Azli Abdul Razak, Masataka Shirakashi, and Norio Arai. "Large eddy simulation of wind pressure distribution on heterogeneous buildings in idealised urban models." *Energy Procedia* 78 (2015): 3055-3060.
[5] Tominaga, Yoshihide, and Bert Blocken. "Wind tunnel experiments on cross-ventilation flow of a generic building with contaminant dispersion in unsheltered and sheltered conditions." *Building and Environment* 92 (2015): 452-461.
[6] Van Hooff, T., and Bert Blocken. "On the effect of wind direction and urban surroundings on natural ventilation of a large semi-enclosed stadium." *Computers & Fluids* 39, no. 7 (2010): 1146-1155.
[7] Shui, Tao Tao, Jing Liu, and Fei Ma. "Numerical simulation of cross-ventilation in buildings affected by surrounding buildings with different separation distances." In *Applied Mechanics and Materials*, vol. 353, pp. 2993-2996. Trans Tech Publications, 2013.
[8] Zaki, Sheikh Ahmad, Aya Hagishima, and Jun Tanimoto. "Experimental study of wind-induced ventilation in urban building of cube arrays with various layouts." *Journal of Wind Engineering and Industrial Aerodynamics* 103 (2012): 31-40.
[9] Cheung, James OP, and Chun-Ho Liu. "CFD simulations of natural ventilation behaviour in high-rise buildings in regular and staggered arrangements at various spacings." *Energy and Buildings* 43, no. 5 (2011): 1149-1158.
[10] Mochida, Akashi, Hiroshi Yoshino, Tomoya Takeda, Toshimasa Kakegawa, and Satoshi Miyauchi. "Methods for controlling airflow in and around a building under cross-ventilation to improve indoor thermal comfort." *Journal of Wind Engineering and Industrial Aerodynamics* 93, no. 6 (2005): 437-449.
[11] Seifert, Joachim, Yuguo Li, James Axley, and Markus Rösler. "Calculation of wind-driven cross ventilation in buildings with large openings." *Journal of Wind Engineering and Industrial Aerodynamics* 94, no. 12 (2006): 925-947.
[12] Karava, P., T. Stathopoulos, and A. K. Athienitis. "Airflow assessment in cross-ventilated buildings with operable façade elements." *Building and Environment* 46, no. 1 (2011): 266-279.
[13] Bangalee, M. Zavid Iqbal, Jiun-Jih Miau, San-Yih Lin, and Mohammad Ferdows. "Effects of lateral window position and wind direction on wind-driven natural cross ventilation of a building: a computational approach." *Journal of Computational Engineering* 2014 (2014).
[14] Ramponi, Rubina, and Bert Blocken. "CFD simulation of cross-ventilation for a generic isolated building: impact of computational parameters." *Building and Environment* 53 (2012): 34-48.
[15] Jiang, Yi, and Qingyan Chen. "Effect of fluctuating wind direction on cross natural ventilation in buildings from large eddy simulation." *Building and Environment* 37, no. 4 (2002): 379-386.
[16] Franke, J., Hellsten, A., Schlünzen, H., Carissimo, B., Guideline for the CFD simulation of flows in the urban environment: *COST Action 732 quality assurance and improvement of microscale meteorological models. Belgium: COST Office*, (2007).
[17] He, Ping, Tadahisa Katayama, Tetsuo Hayashi, Jun-ichiro Tsutsumi, Jun Tanimoto, and Izuru Hosooka. "Numerical simulation of air flow in an urban area with regularly aligned blocks." *Journal of wind engineering and industrial aerodynamics* 67 (1997): 281-291.
[18] Claus, Jean, Omduth Coceal, T. Glyn Thomas, S. Branford, Stephen E. Belcher, and Ian P. Castro. "Wind-direction effects on urban-type flows." *Boundary-layer meteorology* 142, no. 2 (2012): 265-287.

[19] Coceal, O., T. G. Thomas, I. P. Castro, and S. E. Belcher. "Mean flow and turbulence statistics over groups of urban-like cubical obstacles." *Boundary-Layer Meteorology* 121, no. 3 (2006): 491-519.
[20] Santiago, J. L., O. Coceal, A. Martilli, and S. E. Belcher. "Variation of the sectional drag coefficient of a group of buildings with packing density." *Boundary-layer meteorology*128, no. 3 (2008): 445-457.
[21] Yakhot, V. S. A. S. T. B. C. G., S. A. Orszag, S. Thangam, T. B. Gatski, and C. G. Speziale. "Development of turbulence models for shear flows by a double expansion technique." *Physics of Fluids A: Fluid Dynamics* 4, no. 7 (1992): 1510-1520.
[22] Patankar, S., Spalding, D. B., "A calculation procedure for heat, mass and momentum transfer in three-dimensional parabolic flows." *International Journal of Heat and Mass Transfer* 15, no.10 (1972): 1787–1806.
[23] Tominaga, Yoshihide, Akashi Mochida, Ryuichiro Yoshie, Hiroto Kataoka, Tsuyoshi Nozu, Masaru Yoshikawa, and Taichi Shirasawa. "AIJ guidelines for practical applications of CFD to pedestrian wind environment around buildings." *Journal of wind engineering and industrial aerodynamics* 96, no. 10-11 (2008): 1749-1761.
[24] Cermak, Jack E., Michael Poreh, Jon A. Peterka, and Samir S. Ayad. "Wind tunnel investigations of natural ventilation." *Journal of transportation engineering* 110, no. 1 (1984): 67-79.
[25] Blocken, Bert, Ted Stathopoulos, and Jan Carmeliet. "CFD simulation of the atmospheric boundary layer: wall function problems." *Atmospheric environment* 41, no. 2 (2007): 238-252.
[26] Evola, Gianpiero, and Viktor Popov. "Computational analysis of wind driven natural ventilation in buildings." *Energy and buildings* 38, no. 5 (2006): 491-501.
[27] Jiang, Yi, and Qingyan Chen. "Study of natural ventilation in buildings by large eddy simulation." *Journal of Wind engineering and industrial aerodynamics* 89, no. 13 (2001): 1155-1178.
[28] Kim, Yong Chul, Akihito Yoshida, and Yukio Tamura. "Characteristics of surface wind pressures on low-rise building located among large group of surrounding buildings." *Engineering Structures* 35 (2012): 18-28.
[29] van Hooff, Twan, Bert Blocken, and Yoshihide Tominaga. "On the accuracy of CFD simulations of cross-ventilation flows for a generic isolated building: comparison of RANS, LES and experiments." *Building and Environment* 114 (2017): 148-165.
[30] Oke, Tim R. "Street design and urban canopy layer climate." *Energy and buildings* 11, no. 1-3 (1988): 103-113.